

Research Article

Increased susceptibility to dextran sulfate-induced mucositis of iron-overload β -thalassemia mice, another endogenous cause of septicemia in thalassemia

Peerapat Visitchanakun¹, Wimonrat Panpetch¹, Wilasinee Saisorn¹, Piraya Chatthanathon², Dhammika Leshan Wannigama^{1,3,4}, Arthid Thim-uam⁵, Saovaros Svasti⁶, Suthat Fucharoen⁶, Naraporn Somboonna^{2,7} and  Asada Leelahavanichkul^{1,8}

¹Department of Microbiology, Faculty of Medicine, Chulalongkorn University, Bangkok, Thailand; ²Department of Microbiology, Faculty of Science, Chulalongkorn University, Bangkok, Thailand; ³Antimicrobial Resistance and Stewardship Research Unit, Faculty of Medicine, Chulalongkorn University, Bangkok, Thailand; ⁴School of Medicine, Faculty of Health and Medical Sciences, The University of Western Australia, Nedlands, Western Australia, Australia; ⁵Division of Biochemistry, School of Medical Sciences, University of Phayao, Phayao, Thailand; ⁶Thalassemia Research Center, Institute of Molecular Biosciences, Mahidol University, Nakornpathom, Thailand; ⁷Microbiome Research Unit for Probiotics in Food and Cosmetics, Chulalongkorn University, Bangkok, Thailand; ⁸Translational Research in Inflammation and Immunology Research Unit (TRIRU), Department of Microbiology, Chulalongkorn University, Bangkok, Thailand

Correspondence: Asada Leelahavanichkul (aleelahavanit@gmail.com)



Enterocyte damage and gut dysbiosis are caused by iron-overload in thalassemia (Thl), possibly making the gut vulnerable to additional injury. Hence, iron-overload in the heterozygous β -globin deficient (Hbb^{th3/+}) mice were tested with 3% dextran sulfate solution (DSS).

With 4 months of iron-gavage, iron accumulation, gut-leakage (fluorescein isothiocyanate dextran (FITC-dextran), endotoxemia, and tight junction injury) in Thl mice were more prominent than WT mice. Additionally, DSS-induced mucositis in iron-overloaded mice from Thl group was also more severe than the WT group as indicated by mortality, liver enzyme, colon injury (histology and tissue cytokines), serum cytokines, and gut-leakage (FITC-dextran, endotoxemia, bacteremia, and the detection of Green-Fluorescent Producing *Escherichia coli* in the internal organs after an oral administration). However, *Lactobacillus rhamnosus* GG attenuated the disease severity of DSS in iron-overloaded Thl mice as indicated by mortality, cytokines (colon tissue and serum), gut-leakage (FITC-dextran, endotoxemia, and bacteremia) and fecal dysbiosis (microbiome analysis). Likewise, *Lactobacillus* conditioned media (LCM) decreased inflammation (supernatant IL-8 and cell expression of *TLR-4*, nuclear factor κ B (*NF κ B*), and cyclooxygenase-2 (*COX-2*)) and increased transepithelial electrical resistance (TEER) in enterocytes (Caco-2 cells) stimulated by lipopolysaccharide (LPS) and LPS plus ferric ion.

In conclusion, in the case of iron-overloaded Thl, there was a pre-existing intestinal injury that was more vulnerable to DSS-induced bacteremia (gut translocation). Hence, the prevention of gut-derived bacteremia and the monitoring on gut-leakage might be beneficial in patients with thalassemia.

Received: 08 April 2021
Revised: 27 May 2021
Accepted: 08 June 2021

Accepted Manuscript online:
08 June 2021
Version of Record published:
16 June 2021

Introduction

The most common genetic disorder of abnormal hemoglobin synthesis in Asia is β -thalassemia. [1–3]. The β -globin deficiency in β -thalassemia, due to point mutations in the β -globin gene, results in ineffective erythropoiesis, premature death of erythroid progenitor cells, prominent hemolysis, splenomegaly,

and abnormal bone growth [1–3]. Because of the frequent need for blood transfusions, secondary hemochromatosis (iron accumulation in multiple organs or iron-overload) is common in patients with β -thalassemia major. This causes many major complications in patients with thalassemia (Thl) [4]. Among them, several effects of iron-overload on the immune system, including (i) a deterioration in the microbial control mechanisms (chemotaxis and bactericidal activity) of innate immune cells (macrophages and neutrophils) [5,6], (ii) direct toxicity against immune cells, and (iii) increased microbial growth [7,8], may lead to increased susceptibility to infection in patients with Thl.

Furthermore, iron-overload causes injury in Thl enterocytes, which may lead to gut translocation of lipopolysaccharide (LPS) [5], a major component of Gram-negative bacteria (the most common species in the gut) [9,10], and Gram-negative bacteremia [11]. Because of the potential negative effects of iron-overload on the immune system or the gastrointestinal tract, it is likely that iron-overload is a factor that worsens septicemia in Thl patients due to increased bacterial translocation from the gut [11] and a deficit of organismal control [5,6]. Endotoxemia (LPS presentation in the bloodstream) may have a variety of negative effects on patients, since LPS is a potent stimulator of immune cells, triggering a variety of inflammatory responses ranging from changes in vital signs to cytokine storm-induced septic shock [12–14]. The association between the iron toxicity in enterocytes and bacteremia (from gut translocation) is previously discussed only in brief, although iron-overload is a well-known risk factor for bacteremia in patients with Thl [15].

Intestinal injury from iron toxicity in Thl patients can be associated with increased susceptibility to a variety of intestinal injuries, including bacteria and/or toxins in contaminated foods, chemicals, uremic toxins, some medications, and infections [16–20]. Among these damages, infective gastroenteritis is the second most common form of infection in patients with Thl [21] (second only to pneumonia) and it can cause a permeability defect in the gut as well as bacteremia [16]. Indeed, septicemia from Gram-negative bacteria (the dominant gut organisms); including *Klebsiella* spp., *Escherichia coli*, *Salmonella* spp. and *Pseudomonas* spp., is common in patients in the tropical area [11,22], including iron-overloaded Thl [11]. Several of the patients with Gram-negative septicemia might be initiated by gut translocation without symptoms of gastroenteritis [11]. Some of the pathogenic bacteria are normal gut microbiota which are kept in gut by the normal intestinal integrity. With gut mucosal injury in iron-overloaded Thl, the increased susceptibility to gut translocation might increase the incidence of septicemia. Moreover, because of pre-existing inflammation from LPS [12–14] and increased LPS toxicity [5] due to the lack of β -globin antioxidant effects [23,24], septicemia in β -thalassemia patients can be more serious than in patients without underlying disease. Despite multiple indirect correlations between iron-overload and increased susceptibility to intestinal injury in patients with Thl, there is still a lack of direct evaluation between these factors in iron-overloaded Thl. Probiotics, on the other hand, are commercially available live microorganisms that have a variety of health benefits, including improved intestinal integrity and reduced gut-leakage [17,25,26]. However, probiotics are also used less often in patients with Thl.

Hence, we tested the susceptibility to mucosal injury in Thl mice with or without iron-overload using dextran sulfate solution (DSS) in $Hbb^{th3/+}$ mice (the heterozygous β -globin knockout mice) in comparison with wildtype (WT) mice. Additionally, *Lactobacillus rhamnosus* GG, the commercially available probiotics, was evaluated in iron-overloaded Thl mice with DSS and *in vitro* to explore the role of probiotics in thalassemic gut mucosal injury.

Materials and methods

Animals and iron-overload models

The protocol for animal experiments was approved by the Institutional Animal Care and Use Committee of the Faculty of Medicine, Chulalongkorn University, Bangkok, Thailand (SST 04/2561), following the National Institutes of Health (NIH), U.S.A. The heterozygous β -globin knockout mice ($Hbb^{th3/+}$ mice) on C57BL/6 background (Thl) were obtained from Mahidol University, Thailand [27]. WT C57BL/6 mice were purchased from Nomura Siam International (Pathumwan, Bangkok, Thailand). All of mice were worked at animal center, Phayathiwittaya Building, Faculty of Medicine, Chulalongkorn University, Bangkok, Thailand. Oral iron sucrose (Venofer, USP) (10 mg/ dose) or normal saline (NSS) control were administered in 8-week-old male mice three times per week for 4 months to induce iron-overload following previous publications [5,6]. To determine an influence of iron-overload, mice were euthanized with sample collection by cardiac puncture under isoflurane anesthesia. Serum was kept at -80°C until used and internal organs, including liver, duodenum (next to stomach) and ascending colon (next to cecum), were prepared in 10% formalin for histology, in Cryogel (Leica Biosystems, Richmond, IL, U.S.A.) for immunofluorescent staining and at -80°C for iron determination in internal organs. Feces from Thl mice with 4 months of iron administration or NSS control were collected from cecum at euthanizing to evaluate fecal microbiome analysis in Thl with or without iron-overload.

Fecal transfer

Because gut permeability defect (gut-leakage) in iron-overloaded Th1 mice might due to iron-induced gut dysbiosis or the direct mucosal injury from iron-overload [5], the alteration of gut microbiota using feces from iron-overload Th1 mice was performed in comparison with the iron administration. Accordingly, the microbiota alteration in non-iron administered mice (both WT and Th1) using co-housing with oral gavage by feces from iron-overloaded Th1 mice [28] was used. The co-housing procedure was conducted by co-housing a non-iron administered mouse (WT or Th1) with two of 4 months iron-administered Th1 mice (iron gavage was continuing on these two mice) in the same cage (three mice per cage). In parallel, another set of 4 months iron-administered Th1 mice were used as fecal donors for the thrice a week fecal gavage into the co-housed mice (the mice without iron administration) to ensure allocoprophy (the consumption of feces from other mice). For fecal preparation, fecal donor mice were put in metabolic cages (Hatteras Instruments, Cary, NC, U.S.A.) for a few hours to collect feces then the fresh feces were mixed, diluted in phosphate buffer solution (PBS; 0.6 g feces in 1 ml PBS) and orally administered in mice at 20 ml/kg/dose. Of note, iron gavage was continuing on the fecal donor mice. The experimental mice and the fecal donor mice were euthanized at 4 months of the experiment by cardiac puncture under isoflurane anesthesia with sample collection.

DSS-induced colitis model and probiotics

To explore the susceptibility of Th1 or WT mice to the mucosal injury, DSS-induced colitis was performed in mice with 4 months iron administration or control NSS with a previous protocol [29]. Briefly, mouse drinking water was replaced with 3% (w/v; 3 g of DSS in 100 ml water) DSS (Sigma–Aldrich, St. Louis, MO, U.S.A.) in water for 1 week before euthanizing with sample collection by cardiac puncture under isoflurane anesthesia. There was no iron oral gavage during the seventh day of DSS administration. Additionally, the stool consistency was semi-quantitatively evaluated using the following score: 0, normal; 1, soft (soft well-formed stool); 2, loose (soft but not well-formed) and 3, diarrhea (watery stool attached to the mouse anus), as previously published [30]. Because of the well-known benefits of probiotics on gut-leakage and enterocytes [17,25,26], probiotic administration was tested. As such, *L. rhamnosus* GG (Mead-Johnson, Evansville, IN, U.S.A.) at 1×10^9 colony-forming units (CFUs) in 0.5 ml PBS or PBS alone (control) were administered once daily for 7 or 15 days for the short-term parameters or the survival analysis, respectively, in iron-overload Th1 mice (4 months iron gavage) with or without DSS. Mice were euthanized with sample collection at 7 days post-DSS through cardiac puncture under isoflurane anesthesia.

Analysis of mouse samples

The automated biochemistry analyzer (Hitachi 917, Roche Diagnostics, Indianapolis, IN, U.S.A.) was used for hematocrit (Hct) with a micro-hematocrit method. Liver injury and serum cytokines were determined by alanine transaminase (ALT) (EALT-100, BioAssay, Haywood, CA, U.S.A.) and enzyme-linked immunosorbent assay (ELISA) (Pepro-Tech, NJ, U.S.A.), respectively. Serum creatinine was measured by QuantiChrom Creatinine Assay (BioAssay). For blood bacterial burdens, mouse blood samples in several dilutions were directly spread on to blood agar plates (Oxoid, Basingstoke, Hampshire, England) and incubated at 37°C for 24 h before the enumeration of bacterial colonies. Serum endotoxin (LPS) was evaluated by HEK-Blue LPS Detection Kit 2 (InvivoGen, San Diego, CA, U.S.A.). Value less than 0.01 EU/ml was recorded as 0 due to the lower limit of the test. Additionally, organ samples were weighed, thoroughly sonicated, then ferric ion and cytokines in supernatant of the homogeneous tissue were measured using iron assay (Ab83366, Abcam, Cambridge, U.K.) and ELISA test (PeproTech), respectively.

Fecal microbiome analysis

Only the fecal microbiota of Th1 mice, but not that of WT mice, was studied. In the first experimental set, feces from mice (0.25 g each mouse) were divided into two control samples and four fecal gavage (Fe) samples (4 months after iron gavage). In this set, one fecal sample in each group was a combination from two mice of the separated cages. The second set of experiments employed feces from each mouse (0.25 g per animal) for individual microbiome study samples, which included Th1 control, iron-overloaded Th1 with and without DSS, and probiotics-treated mice (7 days post-DSS or probiotics). Mouse feces were collected from the different cages to avoid the influence of allocoprophy on fecal microbiome analysis. Then the microbiota analysis was performed as previously described [5,31]. Briefly, the metagenomic DNA was extracted from the prepared samples using a DNAeasy Kit (Qiagen, Valencia, CA) with DNA quality assessment using Nanodrop spectrophotometry. Universal prokaryotic primers 515F (5'-GTGCCAGCMGCCGCGGTAA-3') and 806R (5'-GGACTACHVGGGT WTCTAAT-3') with appended 50 Illumina adapter and 30 Golay barcode sequences were used for 16S rRNA gene V4 library construction.

Gut-leakage determination

The fluorescein isothiocyanate dextran (FITC-dextran) assay, endotoxemia, bacteremia, and dissemination of the administered Green Fluorescent Producing (GFP) *E. coli* were used to measure gut leakage. The detection of FITC-dextran (a nonabsorbable high molecular weight molecule) in serum with Fluorospectrometer (NanoDrop 3300; Thermo Scientific, Wilmington, DE, U.S.A.) [5] at 3 h after an oral administration of 12.5 mg FITC-dextran (4.4 kDa; FD4) (Sigma–Aldrich) indicates gut permeability defect [5]. Endotoxemia and bacteremia measurements were mentioned above. To further support bacterial translocation from gut, GFP *E. coli* (25922GFP) from the American Type Culture Collection (ATCC, Manassas, VA, U.S.A.) at 1×10^9 CFUs in 0.5 ml PBS were orally administered. Mice were euthanized by cardiac puncture under isoflurane anesthesia at 6 h following GFP *E. coli* gavage, with organs collected in Cryogel (Leica Biosystems) for microscopic fluorescence examination using ZEISS LSM 800 (Carl Zeiss, Berlin, Germany).

Histological analysis and immunofluorescent stain

Mouse organs were fixed in 10% formalin and processed into 4- μ m-thick paraffin-embedded sections before staining with Prussian Blue and Hematoxylin and Eosin (H&E) color to determine iron accumulation in the colon as previously described [5,6]. Briefly, 20% hydrochloric acid with 10% potassium ferrocyanide was used before counterstaining by H&E color, dehydrating in increasing alcohol gradients with Xylene and mounting cover glasses with Resinous Mounting Medium. To quantify iron accumulation in the organs, the intensity and area of Prussian Blue color in the slides were examined under a microscope using ten random fields using ImageJ (NIH, Bethesda, MD, U.S.A.). For determination of DSS-induced colitis, the semi-quantitative evaluation on H&E-stained slides at 200 \times magnification based on mononuclear cell infiltration, epithelial hyperplasia, goblet cell reduction, and epithelial cell vacuolization with the following scores; 0; leukocyte < 5% and no epithelial hyperplasia (<10% of control), 1; leukocyte infiltration 5–10% or hyperplasia 10–25%, 2; leukocyte infiltration 10–25% or hyperplasia 25–50% or reduced goblet cells (>25% of control), 3; leukocyte infiltration 25–50% or hyperplasia >50% or intestinal vacuolization, 4; leukocyte infiltration >50% or ulceration, were used as previously published [25]. For neutrophil count in the ulcer lesions, the neutrophils in ulcer lesions were counted in five randomly selected ulcers per mouse using five randomly selected 400 \times magnification per ulcer. Neutrophil count in the mice without ulcer were scored as 0.

Furthermore, the intestinal tight junctions of ascending colon were evaluated [5] due to the dominant colon injury in DSS-induced mucositis [29]. As such, colon in Cryogel (Leica Biosystems, Richmond, IL, U.S.A.) in 5 μ m-thick acetone-fixed sections were stained by primary antibody against enterocyte tight junction molecules Zona occludens 1 (ZO-1) with secondary green fluorescent antibodies (Alexa Fluor 488) (Life Technologies, Carlsbad, CA, U.S.A.) and visualized (with quantification) by ZEISS LSM 800 (Carl Zeiss).

Impact of *Lactobacillus* conditioned media on LPS-stimulated enterocytes

LPS (a major cell wall component of Gram-negative bacteria) and ferric chloride (FeCl_3) (Sigma–Aldrich) were used *in vitro* to represent the condition in the iron-overloaded intestines due to the high abundance of Gram-negative bacteria and iron-overload in the gut. *Lactobacillus* conditioned media (LCM) was also examined for anti-inflammatory properties on human colonic epithelial cells according to a published procedure [13]. To prepare LCM, *L. rhamnosus* GG at an OD_{600} were cultured anaerobically for 48 h before being centrifuged and concentrated using speed vacuum drying at 40 $^\circ\text{C}$ for 3 h (Savant Instruments, Farmingdale, NY, U.S.A.). The cell-free concentrated pellets were resuspended in an equal volume of Dulbecco's modified Eagle's medium (DMEM) and stored at -20°C until use. Colorectal adenocarcinoma human cells (Caco-2; ATCC HTB-37) were maintained in DMEM at 37 $^\circ\text{C}$ under 5% CO_2 . Caco-2 (2×10^6 cells/well) were incubated, alone or in combination, with LPS (*Escherichia coli* 026: B6) (Sigma–Aldrich) at 100 ng/ml (20 ng/well), FeCl_3 (Sigma–Aldrich) at 200 μM /well, and 5% (vol/vol) (10 μl /well) of LCM from *L. rhamnosus* GG under 5% CO_2 at 37 $^\circ\text{C}$ for 24 h (total volume 200 μl /well). The culture supernatants were prepared by centrifugation (125 $\times g$ at 4 $^\circ\text{C}$ for 7 min), and levels of IL-8 were measured by ELISA (Quantikine immunoassay; R&D Systems, Minneapolis, MN, U.S.A.). Because of the dominant IL-8 production than IL-6 of human Caco-2 epithelial cells, supernatant IL-8, but not IL-6, was quantified in the *in vitro* tests. In addition, gene expression of Toll-like receptor 4 (*TLR4*), nuclear factor κB (*NF\kappa\text{B}*), and Cyclooxygenase-2 (*COX-2*) in Caco-2 were determined by quantitative reverse transcription-PCR (qRT-PCR) with the extracted total RNA using TRIzol reagent (Invitrogen, Carlsbad, CA, U.S.A.). Then, cDNA was prepared from 50 ng of total RNA (SuperScript Vilo cDNA synthesis assay) (Invitrogen) by qPCR instrument (LightCycler 2.0, Roche Diagnostics, Indianapolis, IN, U.S.A.) with the following primers: *TLR4* forward 5'-CAGAACTGCAGGTGCTGG-3'; reverse 5'-GTTCTCTAGAGATGCTAG-3', *NF\kappa\text{B}* forward 5'-CTTCCTCAGCCATGGTACCTCT-3'; reverse 5'-CAAGTCTTCATCAGCATCAAACCTG-3', *COX-2*

forward 5'-CCGGGTACAATCGCACTTAT-3'; reverse 5'-GGCGCTCAGCCATACAG-3', and β -actin forward 5'-CGGTTCCGATGCCCTGAGGCTCTT-3'; reverse 5'-CGTCACACTTCATGATGGAATTGA-3'. The gene expression in relative to the value for β -actin, was calculated according to the $2^{-\Delta\Delta C_T}$ method.

Additionally, several pre-treatments on LCM were conducted before evaluating anti-inflammatory property (supernatant IL-8) on LPS-activated Caco-2 cells in order to identify active compounds in LCM. The enzyme digestion of LCM was tested by incubation with one of various enzymes (Sigma–Aldrich), including α -amylase, lipase, lysozyme, and proteinase K, using 1 mg of enzyme per 1 ml of LCM and incubated at 25°C (for amylase and lysozyme) or 37°C (for lysozyme and proteinase K) for 6 h before enzyme inactivation by heat in a 100°C water bath for 10 min. After that, the treated LCM was tested for IL-8-suppressive activity in a coculture assay with Caco-2 cells (ATCC HTB-37) and LPS (*E. coli* 026: B6) (Sigma–Aldrich) at 100 ng/ml (20 ng/well) as mentioned above. In parallel, LCM thermal stability was assessed by exposing LCM to a 100°C water bath in several durations before use in LPS stimulated Caco-2 cells.

Transepithelial electrical resistance

The integrity of monolayer enterocytes (Caco-2 cells) in different conditions was determined by transepithelial electrical resistance (TEER) according to a previous publication [32]. Briefly, Caco-2 cells (ATCC HTB-37) were seeded on to upper compartment of 24-well Boyden chamber transwell at 5×10^4 cells per well using DMEM-high glucose supplemented with 20% Fetal Bovine Serum (FBS), 1% HEPES, 1% sodium pyruvate, and 1.3% Penicillin/Streptomycin for 15 days to establish confluent monolayer. After that, LPS (*Escherichia coli* 026: B6) (Sigma–Aldrich) at 100 ng/ml (20 ng/well), FeCl₃ (Sigma–Aldrich) at 200 μ M/well and LCM (5%, vol/vol; 10 μ l/well) from *L. rhamnosus* GG were incubated (total volume 200 μ l/well), alone or in combination, under 5% CO₂ at 37°C for 24 h. Then, TEER was measured by an epithelial volt-ohm meter (EVOM-2, World Precision Instruments, Florida, U.S.A.) placing electrodes in supernatant at the basolateral chamber and the apical chamber. The TEER values in media culture without cells was used as a blank and was subtracted from all measurements. The unit of TEER was ohm (Ω) \times cm².

Statistical analysis

Analyzed data using Statistical Package for Social Sciences software (SPSS 22.0, SPSS Inc., IL, U.S.A.) and Graph Pad Prism version 7.0 software (La Jolla, CA, U.S.A.) are presented as mean \pm standard error (SE). The survival analysis was determined by log rank test. The differences between groups were examined for statistical significance by one-way analysis of variance (ANOVA) followed by Tukey's analysis or Student's *t* test for comparisons of multiple or two groups, respectively, and $P < 0.05$ was considered statistically significant.

Results

The more severe iron accumulation in Th1 mice damaged the intestinal tight junction, enhanced severity of DSS-induced mucositis, and resulted in gut translocation of bacteria and septicemia. Hence, the integrity of intestinal mucosa in Th1 should be concerning.

Iron overload-induced intestinal barrier injury and gut dysbiosis in Th1 mice

Characteristics of iron-overload in WT and Th1 mice were evaluated (Figures 1A–I and 2). Iron gavage for 4 months did not improve anemia (Figure 1A) but induced hemochromatosis in Th1 mice, but not in WT, as demonstrated by elevated liver enzyme (ALT) and iron accumulation in organs (liver, duodenum, and colon) with prominent positive Prussian Blue stain in intestinal histology (at serosal area, smooth muscle, and adipocytes) (Figures 1B–E and 2) supported a less severe hemochromatosis in iron-administered WT mice. The prominent secondary hemochromatosis in Th1 mice over WT was indicated by liver injury and iron accumulation in liver as ALT and iron in liver tissue in iron-overloaded mice (Th1+Fe vs. WT+Fe) were 114 ± 17 vs. 34 ± 3 U/l and 112 ± 12 vs. 17 ± 1 ng/mg, respectively (Figure 1B,C). Likewise, the iron toxicity in gut of Th1 mice was severe enough to cause gut leakage as indicated by FITC-dextran assay, endotoxemia, and tight junction injury (Figure 1F–H). Iron accumulation in the colon of Th1+Fe vs. WT+Fe were 48 ± 4 vs. 12 ± 2 ng/mg (Figure 1D, right side), while serum endotoxin level was 0.04 ± 0.01 EU/ml in Th1+Fe vs. non-detectable in WT+Fe (Figure 1G). These data supported the iron-induced gut-leakage in Th1+Fe mice but not in WT+Fe group. Iron gavage caused only mild tight junction injury in WT, as illustrated by immunofluorescent photographs, but no gut leakage as evidenced by other indicators (FITC-dextran and endotoxemia) (Figure 1F–H). Notably, there was no hemochromatosis, systemic inflammation, and gut-leakage in mice without iron gavage

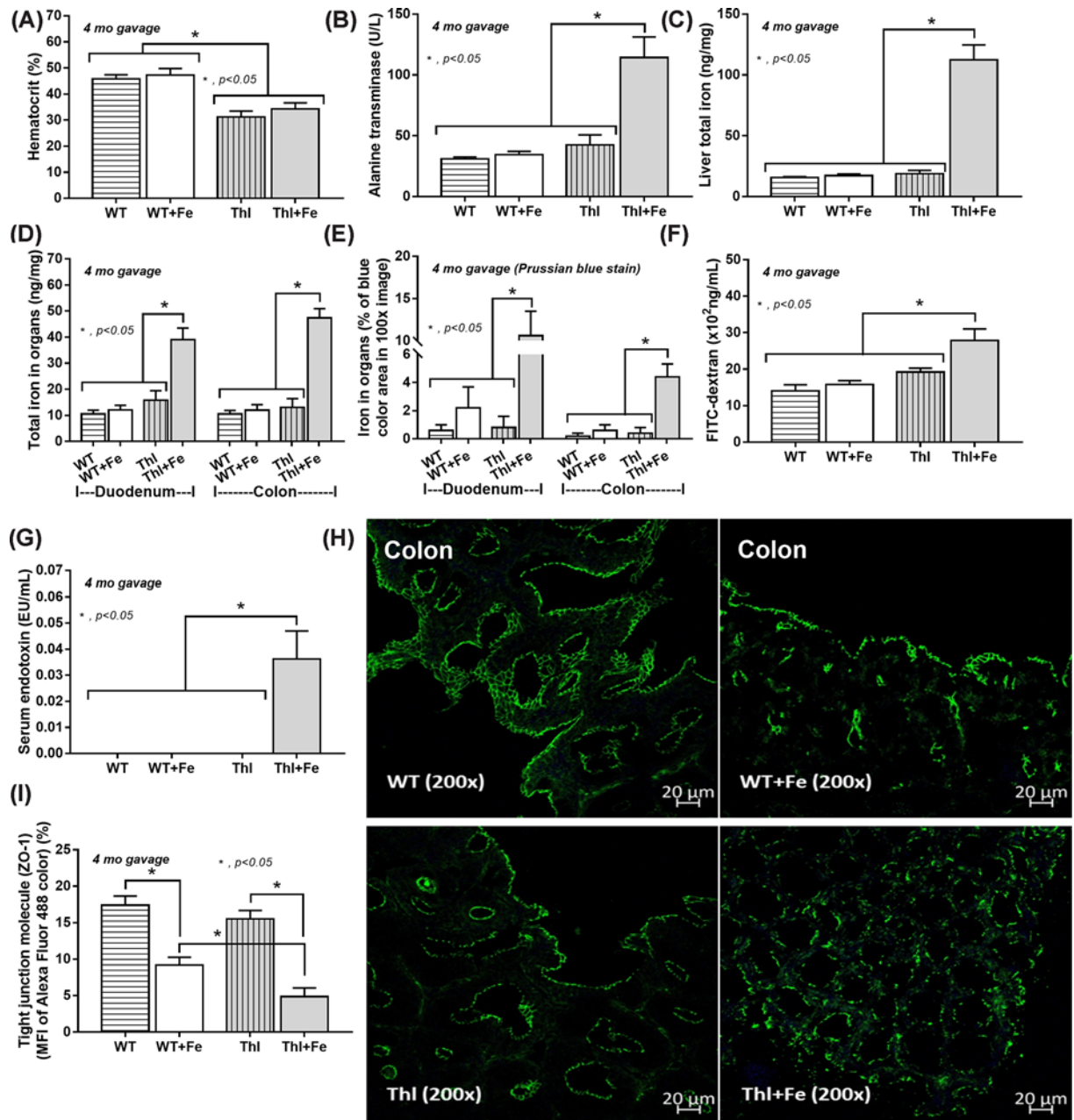


Figure 1. Iron overload and gut permeability defect

Characteristics of iron-overload in WT and Th1 mice as determined by Hct (A), serum ALT (B), iron accumulation in organs (liver, duodenum, and colon) by total iron (C,D) and the score of Prussian Blue stained histology (duodenum and colon) (E) and gut-leakage biomarkers, including FITC-dextran, endotoxemia, and tight junction protein (ZO-1) with the representative immunofluorescent figures (F–I) are demonstrated ($n = 5$ –8/group).

(Th1 and WT) and in iron-administered WT mice (Figure 1B–H) supported the more severe iron complications in Th1 mice [12–14].

However, iron gavage not only affects intestinal injury but also induces gut dysbiosis [33,34]. Because of the less serious hemochromatosis in iron-administered WT mice, only fecal microbiome analysis of Th1 mice, but not of WT mice, was performed (Figure 1B–H). Accordingly, relative to Th1 mice without iron, iron-administered Th1 mice had fecal dysbiosis, with 14 different unique-bacteria (Venn diagram analysis) (Figure 3A–D and Table 1).

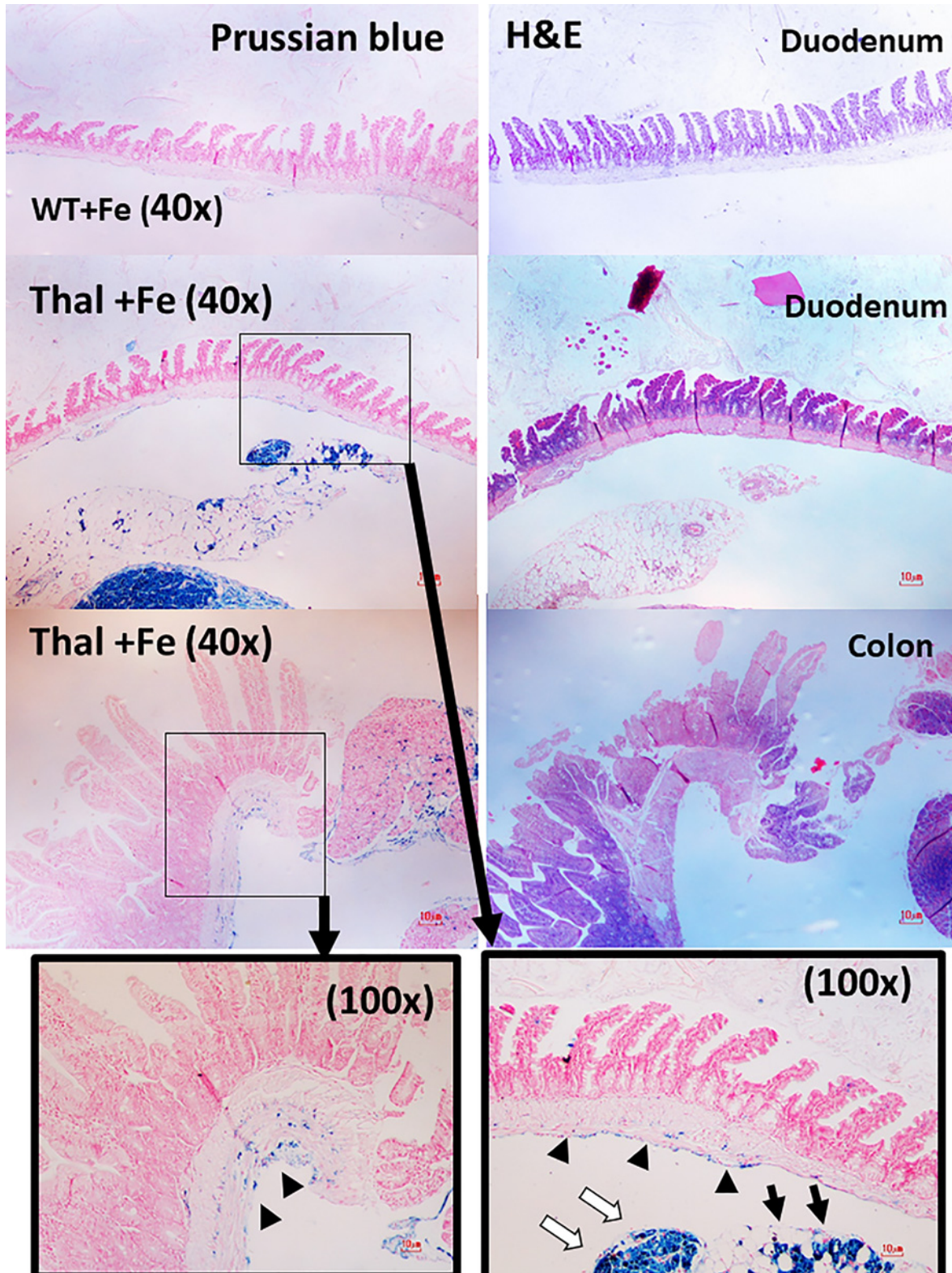


Figure 2. The representative pictures of Prussian Blue and H&E-stained histology of iron-overloaded WT (WT+Fe) and Th1 (Th1+Fe) mice in duodenum and colon are demonstrated

The pictures of colon in WT+Fe and intestines of mice without iron gavage (duodenum and colon) are not shown due to the negative Prussian Blue stain similar to the presented duodenum of WT+Fe. The pictures in 100× magnification demonstrate the Prussian Blue color of iron staining at the serosal area (arrow heads), muscle (white arrows), and omental adipocytes (black arrows).

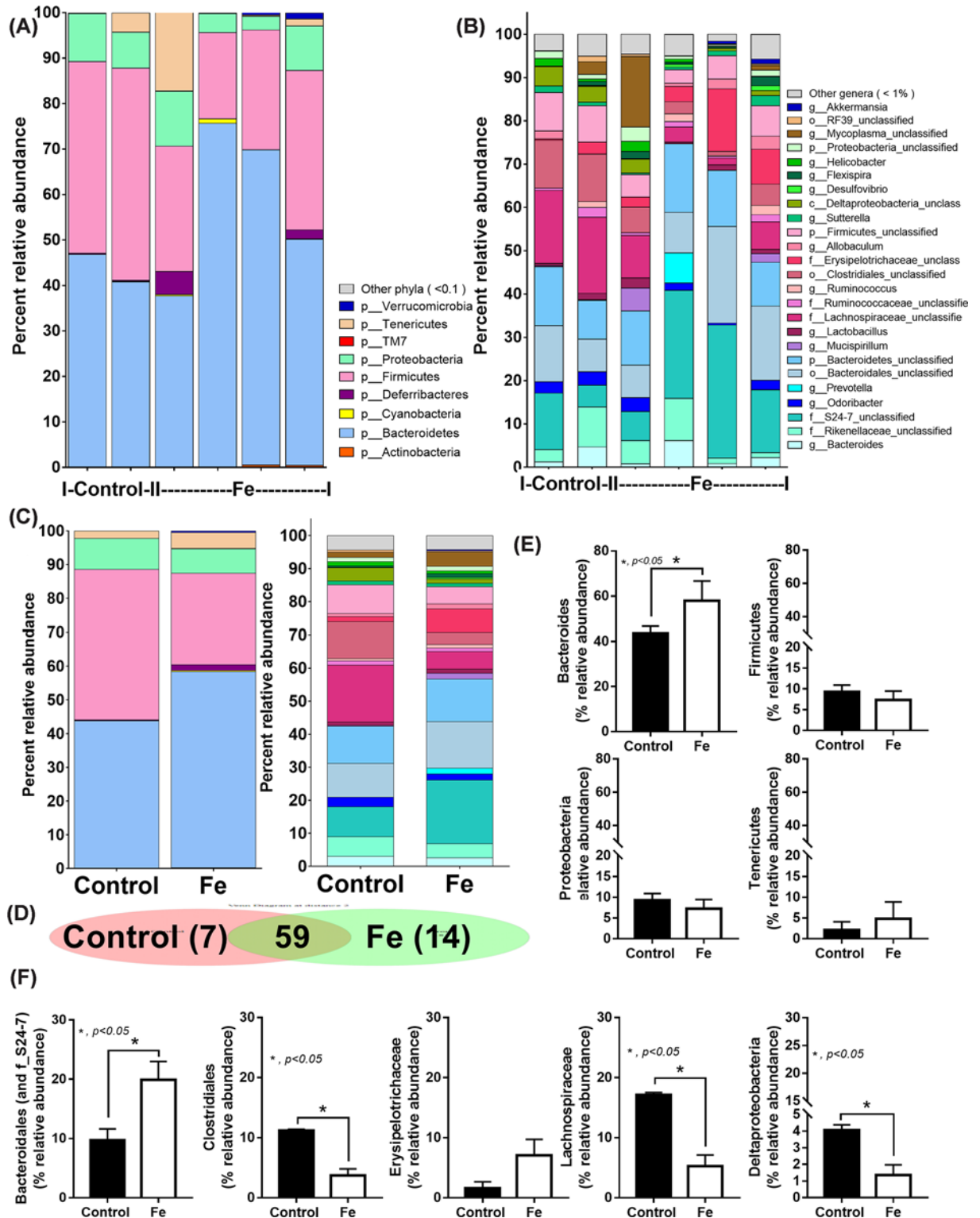


Figure 3. Fecal microbiome analysis of thalassemia mice with iron overload

Gut microbiota analysis from feces of Th1 mice with or without iron gavage (Fe vs. Control) by relative abundance of bacterial diversity at phylum and genus with the average calculation (A–C), Venn diagram with the number of unique bacteria in each group (D), and the graph presentation of the analysis at phylum (E) and at genus level (F) are demonstrated.

Table 1 Unique bacteria (in genus level) from each group (as in Venn diagram)

Control (n=8)	Fe (n=14)
Dehalobacterium (Firmicutes)	Prevotella (Bacteroidetes)
(Spirochaetes)	Akkermansia muciniphila (Verrucomicrobia)
Neisseriaceae (Proteobacteria)	Bifidobacterium (Actinobacteria)
Desulfovibrionales (Proteobacteria)	Butyrivibrio (Firmicutes)
Stenotrophomonas (Proteobacteria)	Olsenella (Actinobacteria)
Streptophyta (Cyanobacteria)	Adlercreutzia (Actinobacteria)
Flavobacteriales (Bacteroidetes)	Bifidobacteriaceae (Actinobacteria)
	Anaerotruncus (Firmicutes)
	Coprobacillus (Firmicutes)
	Haemophilus influenzae (Proteobacteria)
	Butyricimonas (Bacteroidetes)
	Odoribacteraceae (Bacteroidetes)
	(Cyanobacteria)
	Ignatzschineria (Proteobacteria)

Bacterial phyla are identified in ().

Bacteroidales, the Gram-negative pathogenic anaerobes [35], were more abundant in feces of Thl+Fe mice compared with Thl, despite a decrease in bacteria in the order Clostridiales (family Lachnospiraceae), the Gram-positive anaerobic fermenters of plant-polysaccharide in phylum Firmicutes [36], and Deltaproteobacteria, the Gram-negative aerobes with limited virulence [37,38] (Figure 3E,F). The iron-enhanced Bacteroidales was indicated by the percent relative abundance in feces of mice with Thl+Fe vs. Thl were 20 ± 3 vs. $10 \pm 2\%$ (Figure 3F), respectively, supporting the previously reported association between heme and Bacteroides fecal abundance (a heme-dependent characteristic) [34].

Since iron-induced dysbiosis might be associated with mucosal injury, 4 months of fecal transfer procedures (the transplantation of feces from Thl+Fe mice into WT and Thl mice using the co-housing with fecal gavage; see method) was tested in comparison with iron gavage. The allocoprophyagy, a habit of consuming feces from other mice, with fecal gavage, transferred both microbiota and excreted iron from the iron-treated Thl mice to other mice. Nevertheless, fecal transfer did not affect both WT and Thl mice as evaluated by Hct, liver injury (ALT), systemic inflammation (serum IL-6), and gut-leakage (FITC-dextran and endotoxemia) (Figure 4A–E). These findings suggested that fecal dysbiosis had a minor effect on iron-overloaded Thl mice, while iron injury had a greater impact on intestinal injury.

An enhanced severity of DSS-induced colitis in iron-overloaded Thl mice

To see the susceptibility of iron-overloaded enterocytes to mucosal injury, DSS was administered in both WT and Thl mice with or without iron gavage. Accordingly, DSS-induced colitis in iron-administered Thl mice (Thl+Fe DSS) was more severe than iron-treated WT mice (WT+Fe DSS) as determined by a significantly increase in 7 days mortality rate (60 and 10% in mortality rate of Thl+Fe DSS vs. WT+Fe DSS, respectively) while there was no mortality in DSS without iron administration in both mouse strains (WT and Thl) (Figure 5A). The earlier DSS-induced mucosal injury in Thl+Fe DSS mice was indicated by the earlier presentation of loose stool (2–3 days post-DSS) compared with 4–5 days post-DSS in the WT; however, the severity of diarrhea (weight loss and renal function) was not different between groups (Figure 5B–D). Hence, dehydration is not a cause of death in Thl+Fe DSS mice. However, liver enzyme (ALT), serum cytokines (TNF- α and IL-6), cytokines in colon tissue (TNF- α and IL-6) and colon histological score, in Thl+Fe DSS mice was higher than WT+Fe DSS mice (Figures 5E–J and 6) supporting the prominent inflammation in Thl+Fe DSS mice. Although DSS induced more severe injury (with the larger ulcer lesions) in Thl+Fe compared with WT+Fe (intestinal injury score; Figure 5J), the average neutrophil count in each ulcer between Thl+Fe DSS and WT+Fe DSS were similar (Figure 5K). These data implied the similar ulcer characteristics despite the differences in numbers and ulcer area between groups. Of note, the severity of DSS-induced mucosal injury was not different between WT and Thl mice without iron gavage (WT+DSS vs. Thl+DSS) (Supplementary Figure S1A,B) which was not different from WT+Fe DSS (Figure 5J). The less severe injury in iron-overloaded WT mice with DSS (WT+Fe DSS) compared with Thl+Fe DSS mice (Figure 5J) was possibly due to the less prominent iron injury in WT compared with Thl mice (Figures 1D,E and 2).

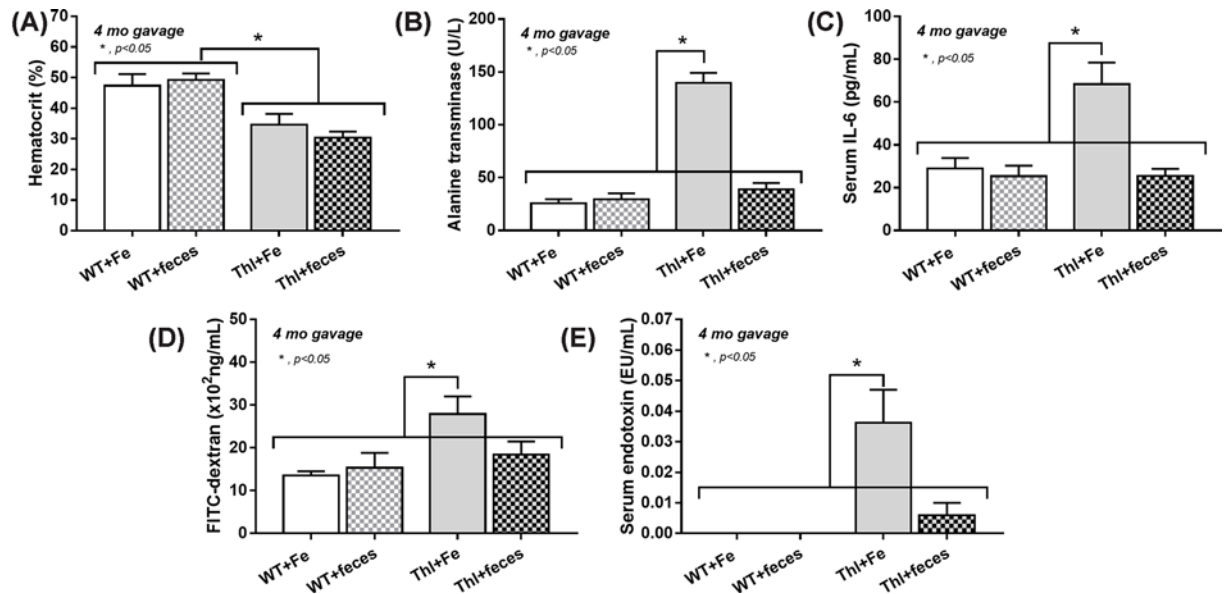


Figure 4. Limited influence of the fecal transfer on the model

Impact of the transfer of feces, co-housing with oral gavage (see method), from iron-overloaded thalassemia (Thl) mice into the non-iron administered mice of both WT (WT+feces) and Thl (Thl+feces) group compared with iron-overloaded mice (WT+Fe and Thl+Fe) as evaluated by Hct (A), liver injury (serum ALT) (B), systemic inflammation (serum IL-6) (C) and gut-leakage (FITC-dextran assay and endotoxemia) (D,E) are demonstrated ($n = 4-6$ /group).

On the other hand, gut-leakage and gut translocation of microbial molecules (FITC-dextran assay, endotoxemia, and bacteremia) was more severe in Thl+Fe DSS mice than WT+Fe DSS mice (Figure 7A–C). Iron-overloaded Thl mice without DSS (Thl+Fe) also demonstrated less severe gut-leakage (FITC-dextran and endotoxemia) when compared with WT+Fe, supported iron-induced intestinal injury [5,6]. The serum endotoxin in WT+Fe DSS was 0.02 ± 0.01 EU/ml, while the level in Thl+Fe and Thl+Fe DSS were 0.03 ± 0.01 and 0.05 ± 0.01 EU/ml, respectively (Figure 7B). In Thl+Fe mice (without DSS), there was no detectable bacteremia (Figure 7C), suggesting that the severity of gut leakage from iron toxicity alone was insufficient to enable gut translocation of viable bacteria. In contrast, bacteremia was detectable in DSS-administered groups (WT and Thl) (Figure 7C). For the further supports on gut translocation of viable bacteria, GFP-*E. coli* was orally administered in iron-treated mice with DSS (WT and Thl). As such, GFP-*E. coli* were demonstrated in mesenteric lymph nodes (MLNs), liver and lung of Thl+Fe DSS mice, while only found in MLN in WT+Fe DSS mice (Figure 7D,E). The fluorescent intensity score of GFP-*E. coli* in MLN of Thl+Fe DSS vs. WT+Fe DSS were 39 ± 6 vs. 4 ± 2 units, respectively (Figure 7D), implying the more prominent gut translocation of bacteria in Thl+Fe DSS.

Probiotics attenuated DSS-induced colitis in iron-overloaded Thl mice through the improved enterocyte functions

L. rhamnosus GG attenuated disease severity of Thl+Fe DSS mice as indicated by survival analysis, stool consistency index, colon inflammation (TNF- α and IL-6 in colon tissue), systemic inflammation (serum IL-6) and gut-leakage (FITC-dextran, endotoxemia, and bacteremia), but not weight loss (Figure 8A–I), supported the intestinal protection of probiotics [16,25,26]. Survival rate (Figure 8A) and bacteremia (Figure 8I) of Thl+Fe DSS without vs. with the probiotics were 50 vs. 81%, respectively, and 1.7 ± 0.3 vs. 0.6 ± 0.3 log of CFU/ml, respectively. Meanwhile, colon IL-6 and serum IL-6 of Thl+Fe DSS without vs. with the probiotics (Figure 8E,F) were 322 ± 66 vs. 187 ± 28 pg/mg tissue, respectively, and 203 ± 15 vs. 104 ± 6 pg/ml, respectively. These data supported the attenuation of bacterial gut translocation in Thl+Fe DSS mice that reduced systemic inflammation and improved mortality rate by probiotics administration. These findings supported probiotics' property to minimize systemic inflammation and increase survival rates in Thl+Fe DSS mice by attenuating bacterial gut translocation. However, the probiotics did not show the beneficial effects on Thl+Fe mice without DSS (Figure 8A–I).

In addition, an impact of probiotics on fecal dysbiosis was demonstrated by fecal microbiome analysis at 7 days post-DSS (Figure 9A–D). Accordingly, iron administration in Thl mice reduced Firmicutes (the high abundant bac-

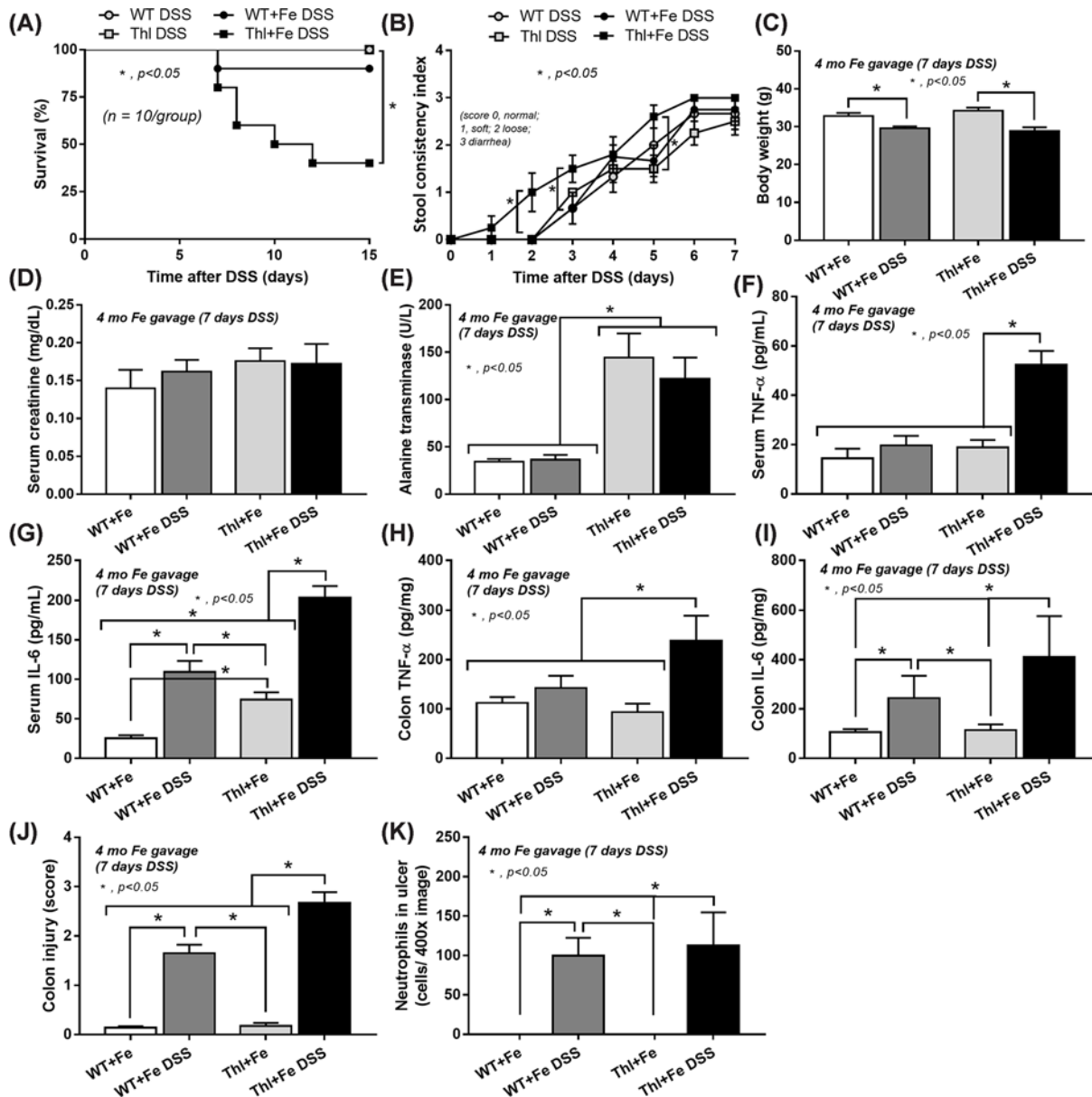


Figure 5. Impact of iron overload on DSS-induced colitis

Characteristics of iron-administered mice with DSS-induced colitis or control drinking water in WT and Th1 mice as determined by survival analysis (A) ($n=10/\text{group}$), stool consistency index (B), and several parameters at 7 days post-DSS or control, including body weight (C), renal injury (serum creatinine) (D), liver enzyme (ALT) (E), systemic inflammation (serum TNF- α and IL-6) (F,G), cytokines in colon tissue (H,I), colon histological score (J) and average neutrophil count in the ulcer lesion (K) are demonstrated ($n=5-7/\text{time-point or group}$ for B-K).

teria in healthy condition [39]) and increased Bacteroides (the Gram-negative anaerobe with pathogenicity in several conditions [17,25,26]) as well as fecal total Gram-negative bacteria (the source of endotoxin in gut contents) (Figure 9E-H). When compared with Th1+Fe without DSS, the abundance of Firmicutes and total Gram-negative bacteria in Th1+Fe DSS was lower and higher, respectively (Figure 9E,H), meaning that fecal dysbiosis was worsened after DSS administration. However, the probiotics attenuated dysbiosis in both Th1+Fe mice and Th1+Fe DSS mice (increased Firmicutes and reduced Bacteroides and decreased total Gram-negative bacteria) (Figure 9E-H). Without DSS (Th1+Fe mice), the probiotics improved fecal dysbiosis in (Figure 9E-H) but did not attenuate iron-induced inflammation in colon (Figure 8D,E) implied a limited impact of gut dysbiosis on intestinal iron toxicity.

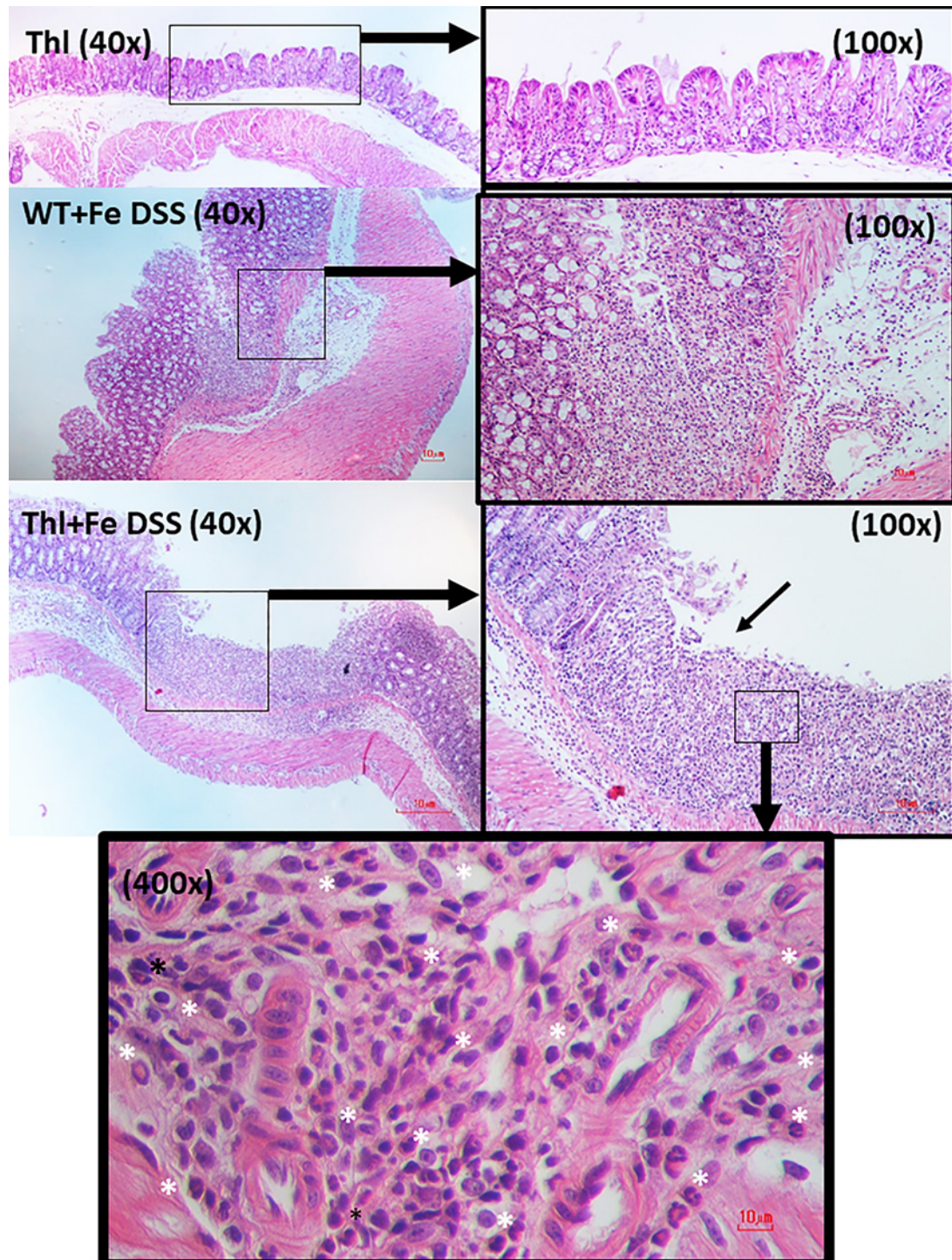


Figure 6. The representative pictures of colon histology on H&E staining of Th1 mice without iron gavage (Th1) (normal histology) and iron-administered mice with DSS-induced colitis in WT (WT+Fe DSS) and Th1 mice (Th1+Fe DSS) are demonstrated. Only pictures of control Th1 mice are demonstrated because of the similarity in gut mucosa between WT and Th1 mice without DSS. The low magnification pictures (40×) indicate the differences in ulcer sizes between WT+Fe DSS and Th1+Fe DSS. Arrows in 100× magnification pictures indicate the ulcer lesions in DSS-administered mice as determined by the loss of villi and the accumulation of inflammatory immune cells in mucosa and submucosa. The higher magnification (400×) is a representative picture indicating generalized neutrophil accumulation in ulcer (the area with neutrophils are presented with 'star symbols' in the 400× picture). Notably, the ulcer in Th1+Fe DSS is larger than WT+Fe DSS despite a similar neutrophil infiltration per area of the ulcer.

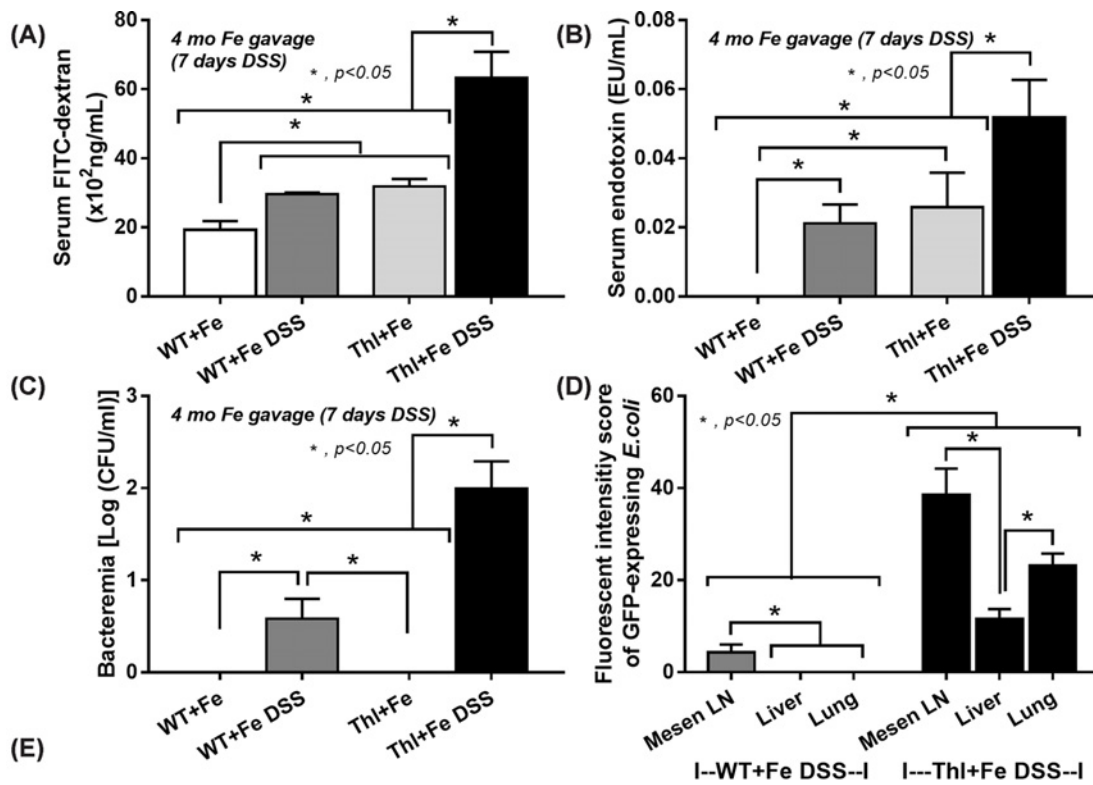


Figure 7. Impact of iron overload on DSS-induced gut permeability defect

Characteristics of iron-administered mice with DSS-induced colitis or control drinking water in WT and Th1 groups as determined by gut-leakage using FITC-dextran assay, endotoxemia, bacteremia (A–C) are demonstrated ($n=5-7$ /group). Additionally, the fluorescent intensity of GFP-expressing *E. coli* in several organs with the representative pictures (D,E) from DSS with iron-administration in both WT and Th1 mice are indicated ($n=5-7$ /group). Of note, (i) the fluorescent intensity score, using the software of confocal microscopy (ZEISS LSM 800, Carl Zeiss), from five random images (200 \times) per organs were used for the presentation (D), (ii) the green fluorescent color of GFP-expressing *E. coli* is most prominent in MLN, and (iii) the pictures of iron-overloaded mice without DSS are not demonstrated due to the negative fluorescence signaling.

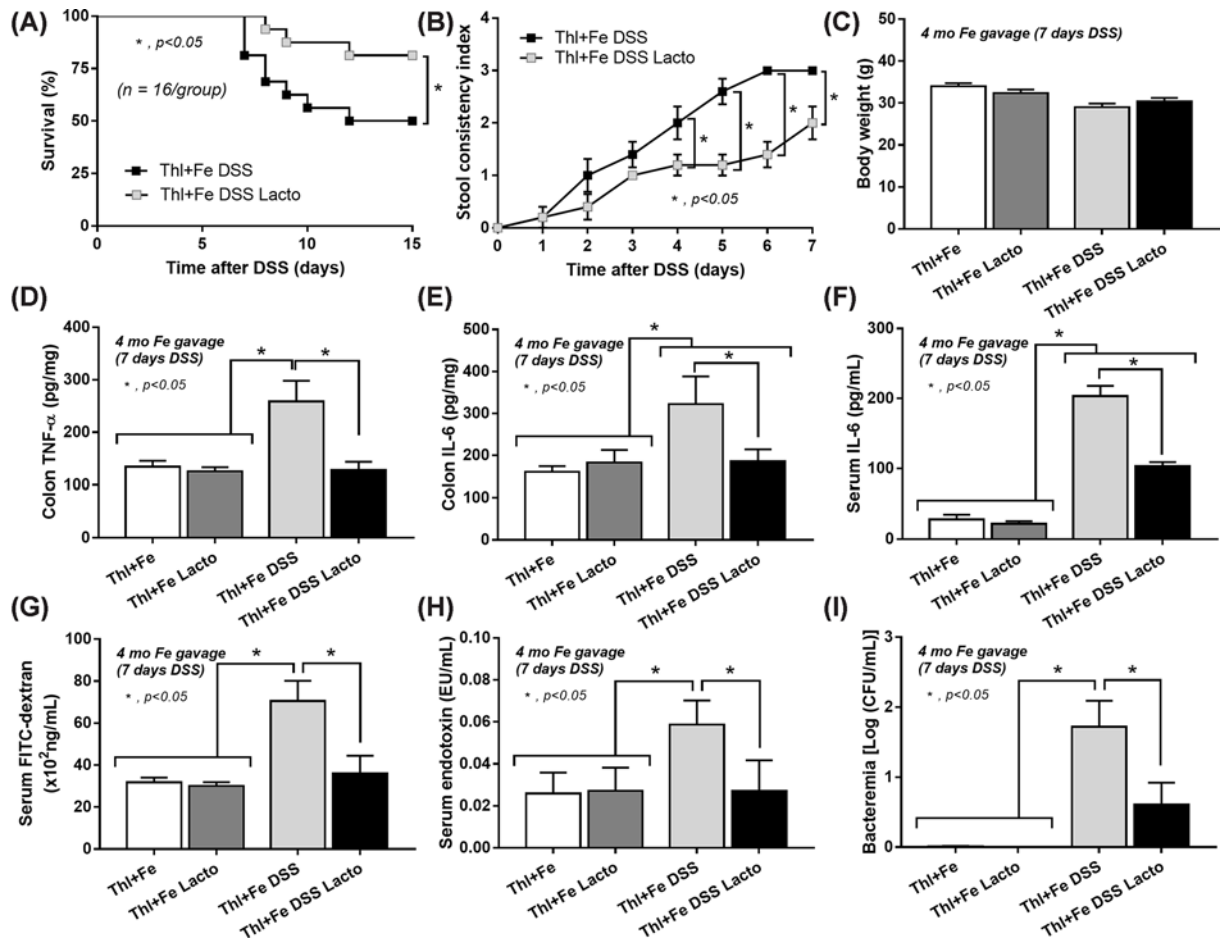


Figure 8. Attenuation of the disease severity by the probiotics

Characteristics of iron-administration with DSS-induced colitis in Th1 mice with or without *L. rhamnosus* (Lacto) as determined by survival analysis (A) ($n=16/\text{group}$), stool consistency index (B) and several parameters at 7 days post-DSS or control, including body weight (C), cytokines from colon tissue (D–F) and gut-leakage (FITC-dextran assay, endotoxemia, and bacteremia) (G–I) are demonstrated ($n=6\text{--}8/\text{time-point}$ or group for B–I).

Moreover, iron was toxic to enterocytes (Caco-2 cells) as indicated by the reduction in TEER (a marker of monolayer cell integrity), but not inflammatory markers (supernatant IL-8 and gene expression of *TLR-4*, *NF κ B* and *COX-2*) (Figure 10A–D). LPS impaired both intestinal integrity (TEER) and induced inflammatory responses which was enhanced by the co-presentation with iron (LPS+Fe) (Figure 10A–D). However, the culture media of *Lactobacilli* (LCM) attenuated inflammatory responses and TEER of the enterocytes after stimulation with either LPS alone or LPS+Fe (Figure 10A–E) supported production the beneficial factors by *L. rhamnosus* GG. Subsequently, LCM was pre-treated with enzyme digestion and heat exposure before being tested against LPS incubation to preliminarily determine active substances in LCM (Figure 10F,G). As such, the anti-inflammatory substances against LPS from *L. rhamnosus* GG contained a polysaccharide structure that was heat stable property (Figure 10F,G) as the anti-inflammatory property was neutralized only by amylase (but not other enzymes) and not by the pre-heat exposure (Figure 10F,G). Hence, our data suggest that *L. rhamnosus* GG may be of interest for the intestinal anti-inflammation.

Discussion

DSS-induced mucositis in Th1 mice was exacerbated by an intestinal barrier defect triggered by iron toxicity, which resulted in gut bacterial translocation and septicemia. *L. rhamnosus* GG attenuated DSS-induced sepsis in Th1 mice, presumably by producing protective factors, and may be a promising candidate for gut mucosal integrity maintenance in Th1.

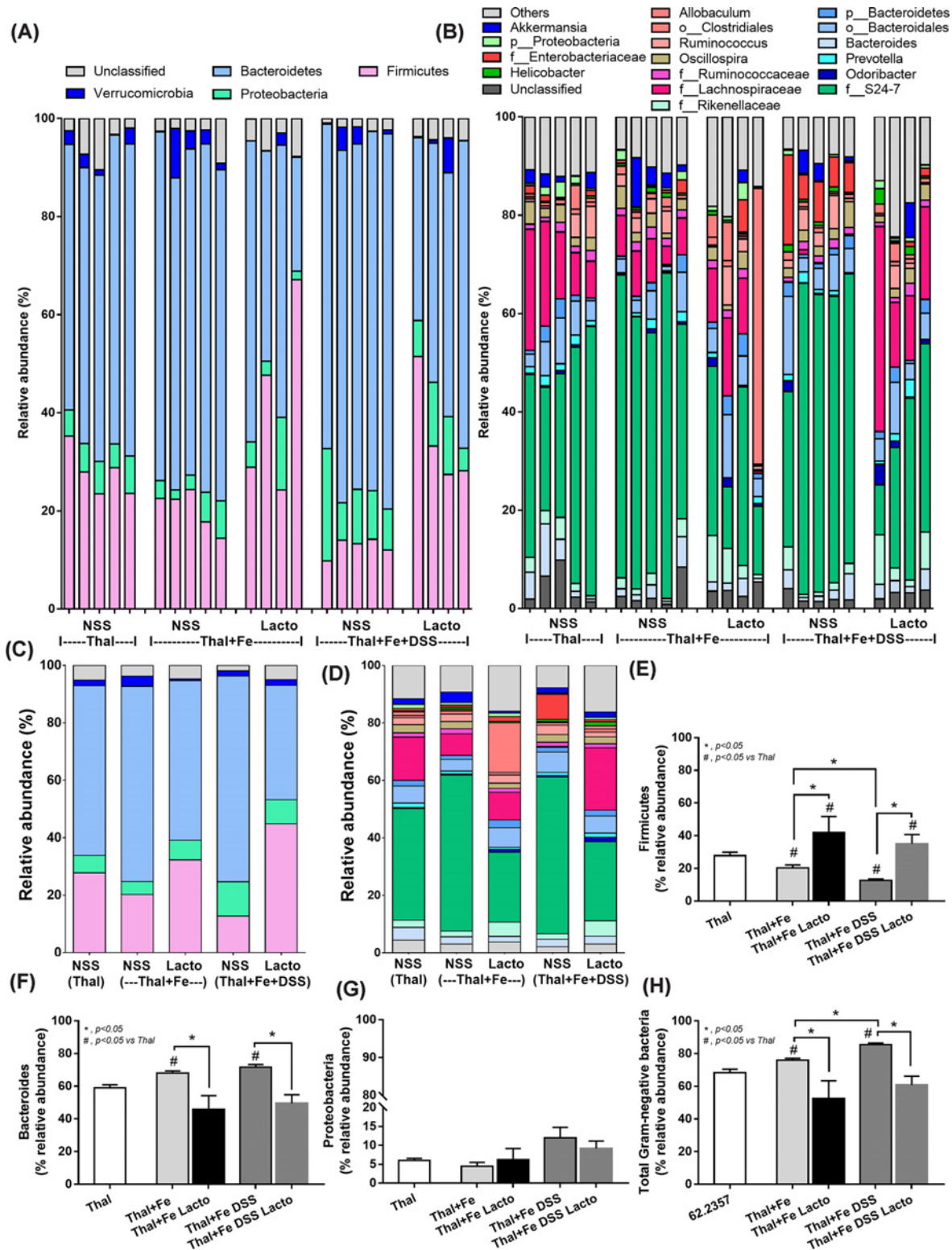


Figure 9. Fecal microbiome analysis with the probiotics administration

Gut microbiota analysis from feces of control thalassemia mice (Thl) with normal saline gavage (NSS), iron-administered Thl mice with NSS (Thl+Fe) or *Lactobacilli* (Thl+Fe Lacto) and DSS-administered iron gavage Thl mice with NSS (Thl+Fe DSS) or *Lactobacilli* (Thl+Fe DSS Lacto) as determined by relative abundance of bacterial diversity at phylum and genus levels with the average calculation (A–D) and the graph presentation of the analysis at phylum (Firmicutes, Bacteroides, and Proteobacteria) (E–G) with total Gram-negative bacterial abundance in feces as calculated from the microbiome analysis in phylum level (H) are demonstrated.

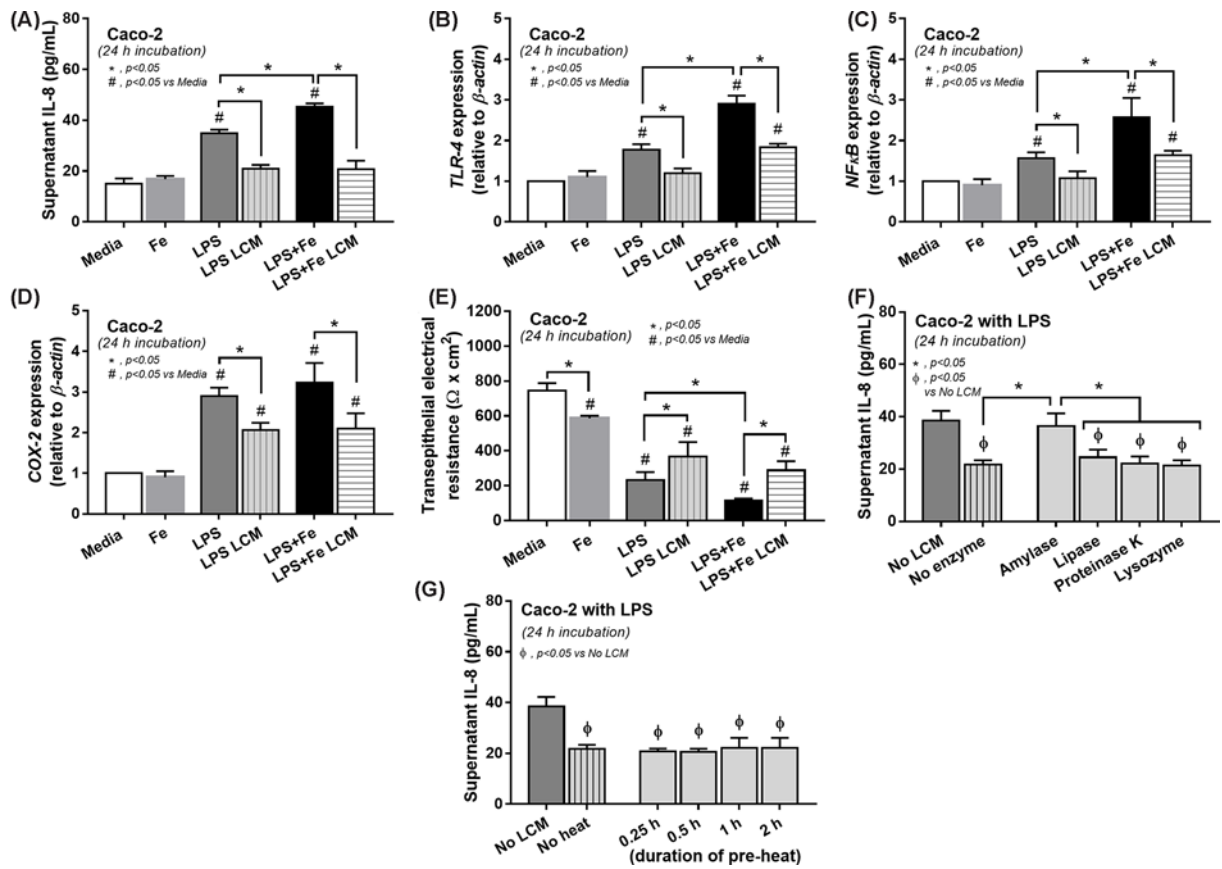


Figure 10. The therapeutic effect of Lactobacillus condition media

Characteristic of enterocytes (Caco-2 cells) after incubation with endotoxin (LPS), ferric ion (Fe), LPS with ferric iron (LPS+Fe) and LCM incubated with LPS (LPS LCM) or LPS+Fe (LPS+Fe LCM) as determined by supernatant cytokine (IL-8) (A) and gene expression of the downstream molecular signals (*TLR-4* and *NFκB*) (B,C) and an inflammatory indicator (*COX-2*) (D) with TEER (E) are demonstrated. Additionally, the impact of LCM after enzyme digestion and heat exposure in several duration before use (pre-heat) in comparison with controls (no LCM, no enzyme, or no pre-heat) are also demonstrated (F,G) (independent triplicated experiments were performed for the *in vitro* experiments).

Iron-overload had a greater effect on gut mucosal injury in iron-overload Th1 mice than dysbiosis

In Th1 mice, iron gavage combined with the rapid degradation of defective red blood cells caused more extreme iron accumulation than in WT mice [5,6], comparable with secondary hemochromatosis in patients [1–4]. Although iron accumulation in intestinal histology was mostly visible in smooth muscle and omental adipocytes (but not in the intestinal villi), iron administration caused a defect in the intestinal tight junction barrier in both Th1 and WT mice.

Since the single cell layer of enterocytes serves as an essential barrier between gut contents and blood circulation, a tight junction defect allows organismal molecules to pass through the gut [14]. However, the tight junction injury was observable by fluorescent staining in iron-overloaded WT mice that did not have leaky gut or endotoxemia, implying that gut leakage occurs only in serious tight junction injuries. Meanwhile, FITC-dextran assay and spontaneous endotoxemia revealed that the tight junction injury in iron-overloaded Th1 mice was serious enough to induce gut leakage. Perhaps, the more prominent intestinal epithelium shedding for enhancing iron disposal [40] in iron-overloaded Th1 mice induced more severe enterocyte injury than WT mice [9,10]. As a result, this pre-existing intestinal injury in iron-overloaded Th1 mice exacerbated the injury caused by DSS, a common substance used in rodent colitis models [29], as evidenced by earlier diarrhea, more serious colon histology, gut-leakage, and a higher mortality rate when compared with WT mice.

Meanwhile, the lower iron-accumulation in WT mice, as indicated by hemochromatosis in liver, induced only a less severe intestinal mucosal injury (reduced tight junction molecules but not induced gut-leakage). In iron-overloaded

Thl mice, the mucosal injury was serious enough to allow gut translocation of endotoxin, a potent pro-inflammatory organismal molecule produced by Gram-negative bacteria, but not viable bacteria. Because the intestinal injury in iron-overload Thl mice might not only due to direct iron toxicity but also iron-induced gut dysbiosis [33,34], fecal microbiome analysis was performed. In Thl mice, iron increased *Bacteroides* spp., Gram-negative bacteria that are major sources of LPS in gut contents, and decreased some anaerobic Gram-positive bacteria in Firmicutes group (Lachnospiraceae and Clostridiales), which are potentially beneficial gut organisms [39]. However, iron-induced gut dysbiosis had a lower effect on mucosal injury in Thl mice than direct iron toxicity, as the transfer of feces (from iron-overloaded Thl mice) for 4 months (using co-housing with fecal gavage) into Thl or WT mice did not cause gut injury. As a result, the direct effect of iron on mucosal injury was greater than the effect of iron on gut dysbiosis.

Septicemia induced by DSS-induced mucosal injury in iron-overload Thl mice, an impact of the pre-existing gut mucosal injury

The susceptibility to infection of patients with Thl is well-known [15]. Here, endotoxemia was demonstrated only in iron-overloaded Thl mice but not in WT highlighting the more severe iron-induced gut mucosal injury in Thl mice. With DSS-induced mucosal injury, bacteremia and gut translocation of GFP-*E. coli* after an oral administration was more prominent in iron-overload Thl mice than in WT mice. As such, GFP-*E. coli* were presented only in MLNs in iron-overloaded WT mice, while presented in several organs with the higher fluorescent intensity in iron-overloaded Thl mice. These implied a more severe DSS-induced gut injury in mice with a higher iron burden. Additionally, the mortality of iron-overloaded Thl mice with DSS (Thl+Fe DSS) was higher than that of WT mice, with higher systemic inflammation and bacteremia, but comparable diarrheal severity, indicated sepsis as the cause of death in Thl+Fe DSS mice. Indeed, several sepsis-worsening factors in Thl have been reported, including impaired immune responses to bacteremia [41,42], delayed neutrophil maturation [27], hypercytokine production [5,6] and chronic inflammatory condition [43], possibly due to a defect in β -globin's ability to neutralize iron-derived oxidants [23,24]. Pre-existing inflammation in Thl can also play a role in the more severe sepsis, as shown by the '2 hits sepsis model' [44,45] and the pre-conditioning inflammation causes more severe sepsis [12–14]. As a result, severe septicemia in Thl+Fe DSS mice could be caused by gut translocation of viable bacteria with defects in microbial control and hyperactive cytokines.

Attenuation of mucosal injury in iron-overload thalassemia mice with DSS, a proposed clinical translation

Because gut translocation is a main pathogenesis of septicemia in iron-overloaded Thl mice and the intestinal protection of probiotics is well-known [25], an attenuation of gut translocation using probiotics might be a direct therapeutic strategy. Indeed, *L. rhamnosus* GG, the commercially available probiotics, attenuated DSS-induced mucositis possibly through the improved gut dysbiosis in iron-overload Thl mice either with or without DSS. However, the probiotics attenuate gut leakage only in the mice with DSS, but not in the mice without DSS. Perhaps, gut leakage in DSS depended on gut dysbiosis more than in iron-overload, as the dysbiosis was more prominent in DSS when compared with iron-overloaded model. Here, iron-overload in Thl mice (Thl+Fe) reduced fecal Firmicutes, bacteria of the healthy condition [39], and increased total Gram-negative bacteria, the source of LPS in gut contents, (compared with Thl control) and the addition of DSS (Thl+Fe DSS) further reduced Firmicutes and increased total Gram-negative bacteria (Figure 9E,H). Since DSS has a more severe gut dysbiosis than iron-overload, attenuating gut dysbiosis in DSS has a more beneficial impact. More studies for the direct comparison between these models are interesting.

Additionally, high dose of ferric ion (Fe^{3+}), a less toxic oxidized trivalent form than ferrous ion (Fe^{2+}) [46] that is systemically transported in the body, was used to test the influence of iron upon enterocytes. Interestingly, the additive effect of ferric iron on LPS in enterocyte injury (the electrical resistance and inflammatory markers) supported the adverse effect of high iron status in responses to organismal molecules [47]. However, after activation with either LPS alone or LPS plus iron, *L. rhamnosus* GG culture media reduced enterocyte damage, presumably due to the excretion of enterocyte protective factors, which have previously been known as exopolysaccharides or lipids [13,16,17,25,26,48,49]. Here, the anti-inflammatory substances against LPS from *L. rhamnosus* GG was identified as the heat-stable exopolysaccharide because the anti-inflammatory effect was neutralized only by amylase. Despite the preliminary experimental study, our preliminary findings support the function of *L. rhamnosus* GG in maintaining intestinal barrier in iron-overload thalassemia. Further studies using probiotics for the prevention of intestinal integrity defect in patients with iron-overload thalassemia are interesting.

In conclusion, when compared with WT mice, intestinal iron accumulation in Thl mice caused pre-existing tight junction injury, resulting in more severe DSS mucositis and gut translocation of viable bacteria, which may progress to severe sepsis in Thl mice due to defects in microbial control and more severe gut-leakage mediated inflammation.

Because septicemia in Th1+Fe DSS mice was attenuated by probiotics, gut-leakage attenuation and evaluation of gut mucosal integrity in patients with iron-overload Th1 might be beneficial.

Clinical perspectives

- **Background:** While hemochromatosis is a well-known complication of Th1, information on the clinical significance of iron accumulation in the intestines is still limited.
- **A brief summary of results:** The increased susceptibility to DSS-induced bacteremia in iron-overloaded Th1 mice (heterozygous β -globin deficiency; Hbb^{th3/+}) compared with WT mice suggested a potential ‘gut-derived sepsis’ in iron-overloaded Th1. The ability of probiotics to attenuate DSS-induced bacteremia in iron-overloaded Th1 mice, presumably due to anti-inflammatory exopolysaccharide substances, supported a possible benefit of probiotics in patients with iron-overloaded Th1.
- **The potential significance of the results to human health and disease:** Due to the increased susceptibility to gut-derived septicemia, which may be responsible for the increased prevalence of sepsis, the monitoring of gut permeability defect (and/or endotoxemia) and the use of probiotics in patients with iron-overloaded Th1 was suggested.

Data Availability

All supporting data are included within the main article and available by contacting the corresponding author.

Competing Interests

The authors declare that there are no competing interests associated with the manuscript.

Funding

This work was supported by the Thailand Research Fund [grant number RES.61.202.30.022]; the Ratchadapisek Sompoch [grant number CU_GR.63.108.3]; the Program Management Unit for Human Resources and Institutional Development Research and Innovation-CU [grant numbers Global Partnership B16F630071 and Flagship B05F630073]; the TSRI Fund [grant number CU_FRB640001.01.23.1]; the Second Century Fund (C2F) Chulalongkorn University; and the National Research Council of Thailand (NRCT) [grant number NRCT5-RGJ63001].

CRedit Author Contribution

Peerapat Visitchanakun: Resources, Data curation, Formal analysis, Methodology. **Wimonrat Panpetch:** Resources, Data curation, Software. **Wilasinee Saisorn:** Resources, Data curation. **Piraya Chatthanathon:** Resources, Data curation. **Dhammika Leshan Wannigama:** Resources. **Arthid Thim-uam:** Resources, Data curation. **Saovaros Svasti:** Resources, Data curation, Formal analysis. **Suthat Fucharoen:** Resources. **Naraporn Somboonna:** Resources, Data curation. **Asada Leelahavanichkul:** Conceptualization, Funding acquisition, Writing—original draft, Project administration, Writing—review and editing.

Abbreviations

ALT, alanine transaminase; ATCC, American Type Culture Collection; CFU, colony-forming unit; COX-2, cyclooxygenase-2; DSS, dextran sulfate solution; ELISA, enzyme-linked immunosorbent assay; FeCl₃, ferric chloride; FITC-dextran, fluorescein isothiocyanate dextran; GFP, green fluorescent producing; Hct, hematocrit; H&E, Hematoxylin and Eosin; LCM, *Lactobacillus* conditioned media; LPS, lipopolysaccharide; MLN, mesenteric lymph node; NF κ B, nuclear factor κ B; NIH, National Institutes of Health; PBS, phosphate buffer solution; TEER, transepithelial electrical resistance; Th1, thalassemia; TLR4, Toll-like receptor 4; WT, wildtype.

References

- 1 Rivella, S. (2009) Ineffective erythropoiesis and thalassemias. *Curr. Opin. Hematol.* **16**, 187–194, <https://doi.org/10.1097/MOH.0b013e32832990a4>
- 2 Fucharoen, S. and Winichagoon, P. (2012) New updating into hemoglobinopathies. *Int. J. Lab. Hematol.* **34**, 559–565, <https://doi.org/10.1111/j.1751-553X.2012.01446.x>
- 3 Rachmilewitz, E.A. and Giardina, P.J. (2011) How I treat thalassemia. *Blood* **118**, 3479–3488, <https://doi.org/10.1182/blood-2010-08-300335>

- 4 Taher, A.T. and Saliba, A.N. (2017) Iron overload in thalassemia: different organs at different rates. *Hematol. Am. Soc. Hematol. Educ. Prog.* **2017**, 265–271, <https://doi.org/10.1182/asheducation-2017.1.265>
- 5 Visitchanakun, P., Saisorn, W., Wongphoom, J., Chatthanathon, P., Somboonna, N., Svasti, S. et al. (2020) Gut leakage enhances sepsis susceptibility in iron-overloaded β -thalassemia mice through macrophage hyperinflammatory responses. *Am. J. Physiol. Gastrointest. Liver Physiol.* **318**, G966–G979, <https://doi.org/10.1152/ajpgi.00337.2019>
- 6 Sae-Khow, K., Charoensappakit, A., Visitchanakun, P., Saisorn, W., Svasti, S., Fucharoen, S. et al. (2020) Pathogen-associated molecules from gut translocation enhance severity of cecal ligation and puncture sepsis in iron-overload beta-thalassemia mice. *J. Inflamm. Res.* **13**, 719–735, <https://doi.org/10.2147/JIR.S273329>
- 7 Khan, F.A., Fisher, M.A. and Khakoo, R.A. (2007) Association of hemochromatosis with infectious diseases: expanding spectrum. *Int. J. Infect. Dis.* **11**, 482–487, <https://doi.org/10.1016/j.ijid.2007.04.007>
- 8 Moura, E., Noordermeer, M.A., Verhoeven, N., Verheul, A.F. and Marx, J.J. (1998) Iron release from human monocytes after erythrophagocytosis in vitro: an investigation in normal subjects and hereditary hemochromatosis patients. *Blood* **92**, 2511–2519, <https://doi.org/10.1182/blood.V92.7.2511>
- 9 Fang, S., Yu, X., Ding, H., Han, J. and Feng, J. (2018) Effects of intracellular iron overload on cell death and identification of potent cell death inhibitors. *Biochem. Biophys. Res. Commun.* **503**, 297–303, <https://doi.org/10.1016/j.bbrc.2018.06.019>
- 10 Fang, S., Zhuo, Z., Yu, X., Wang, H. and Feng, J. (2018) Oral administration of liquid iron preparation containing excess iron induces intestine and liver injury, impairs intestinal barrier function and alters the gut microbiota in rats. *J. Trace Elem. Med. Biol.* **47**, 12–20, <https://doi.org/10.1016/j.jtemb.2018.01.002>
- 11 Teawtrakul, N., Jetsrisuparb, A., Sirirerachai, C., Chansung, K. and Wanitpongpan, C. (2015) Severe bacterial infections in patients with non-transfusion-dependent thalassemia: prevalence and clinical risk factors. *Int. J. Infect. Dis.* **39**, 53–56, <https://doi.org/10.1016/j.ijid.2015.09.001>
- 12 Issara-Amphorn, J., Surawut, S., Worasilchai, N., Thim-Uam, A., Finkelman, M., Chindamporn, A. et al. (2018) The synergy of endotoxin and (1 \rightarrow 3)-beta-D-glucan, from gut translocation, worsens sepsis severity in a lupus model of Fc gamma receptor IIb-deficient mice. *J. Innate Immun.* **10**, 189–201, <https://doi.org/10.1159/000486321>
- 13 Panpetch, W., Chanchaoentana, W., Bootdee, K., Nilgate, S., Finkelman, M., Tumwasorn, S. et al. (2018) Lactobacillus rhamnosus L34 attenuates gut translocation-induced bacterial sepsis in murine models of leaky gut. *Infect. Immun.* **86**, e00700–e00717
- 14 Amornphimoltham, P., Yuen, P.S.T., Star, R.A. and Leelahavanichkul, A. (2019) Gut leakage of fungal-derived inflammatory mediators: part of a gut-liver-kidney axis in bacterial sepsis. *Dig. Dis. Sci.* **64**, 2416–2428, <https://doi.org/10.1007/s10620-019-05581-y>
- 15 Vento, S., Cainelli, F. and Cesario, F. (2006) Infections and thalassaemia. *Lancet Infect. Dis.* **6**, 226–233, [https://doi.org/10.1016/S1473-3099\(06\)70437-6](https://doi.org/10.1016/S1473-3099(06)70437-6)
- 16 Panpetch, W., Kullapanich, C., Dang, C.P., Visitchanakun, P., Saisorn, W., Wongphoom, J. et al. (2021) Candida administration worsens uremia-induced gut leakage in bilateral nephrectomy mice, an impact of gut fungi and organismal molecules in uremia. *mSystems* **6**, e01187–20, <https://doi.org/10.1128/mSystems.e01187-20>
- 17 Panpetch, W., Somboonna, N., Bulan, D.E., Issara-Amphorn, J., Finkelman, M., Worasilchai, N. et al. (2017) Oral administration of live-or heat-killed *Candida albicans* worsened cecal ligation and puncture sepsis in a murine model possibly due to an increased serum (1 \rightarrow 3)- β -D-glucan. *PLoS ONE* **12**, e0181439, <https://doi.org/10.1371/journal.pone.0181439>
- 18 Leelahavanichkul, A., Worasilchai, N., Wannalerdsakun, S., Jutivorakool, K., Somparn, P., Issara-Amphorn, J. et al. (2016) Gastrointestinal leakage detected by serum (1 \rightarrow 3)-beta-D-glucan in mouse models and a pilot study in patients with sepsis. *Shock* **46**, 506–518, <https://doi.org/10.1097/SHK.0000000000000645>
- 19 Bhunyakarnjanarat, T., Udornpompitak, K., Saisorn, W., Chantraprapawat, B., Visitchanakun, P., Dang, C.P. et al. (2021) Prominent indomethacin-induced enteropathy in Fc γ RIIb deficient lupus mice: an impact of macrophage responses and immune deposition in gut. *Int. J. Mol. Sci.* **22**, 1377, <https://doi.org/10.3390/ijms22031377>
- 20 Udornpompitak, K., Bhunyakarnjanarat, T., Charoensappakit, A., Dang, C.P., Saisorn, W. and Leelahavanichkul, A. (2021) Lipopolysaccharide-enhanced responses against aryl hydrocarbon receptor in Fc γ RIIb-deficient macrophages, a profound impact of an environmental toxin on a lupus-like mouse model. *Int. J. Mol. Sci.* **22**, 4199, <https://doi.org/10.3390/ijms22084199>
- 21 Rahav, G., Volach, V., Shapiro, M., Rund, D., Rachmilewitz, E.A. and Goldfarb, A. (2006) Severe infections in thalassaemic patients: prevalence and predisposing factors. *Br. J. Haematol.* **133**, 667–674, <https://doi.org/10.1111/j.1365-2141.2006.06082.x>
- 22 Wanachiwanawin, W. (2000) Infections in E-beta thalassemia. *J. Pediatr. Hematol. Oncol.* **22**, 581–587, <https://doi.org/10.1097/00043426-200011000-00027>
- 23 Liu, L., Zeng, M. and Stamler, J.S. (1999) Hemoglobin induction in mouse macrophages. *Proc. Natl. Acad. Sci. U.S.A.* **96**, 6643–6647, <https://doi.org/10.1073/pnas.96.12.6643>
- 24 Saha, D., Patgaonkar, M., Shroff, A., Ayyar, K., Bashir, T. and Reddy, K.V. (2014) Hemoglobin expression in nonerythroid cells: novel or ubiquitous? *Int. J. Inflamm.* **2014**, 803237, <https://doi.org/10.1155/2014/803237>
- 25 Panpetch, W., Hiengrath, P., Nilgate, S., Tumwasorn, S., Somboonna, N., Wilantho, A. et al. (2020) Additional *Candida albicans* administration enhances the severity of dextran sulfate solution induced colitis mouse model through leaky gut-enhanced systemic inflammation and gut-dysbiosis but attenuated by *Lactobacillus rhamnosus* L34. *Gut Microbes* **11**, 465–480, <https://doi.org/10.1080/19490976.2019.1662712>
- 26 Panpetch, W., Sawaswong, V., Chanchaem, P., Ondee, T., Dang, C.P., Payungporn, S. et al. (2020) Corrigendum: *Candida* administration worsens cecal ligation and puncture-induced sepsis in obese mice through gut dysbiosis enhanced systemic inflammation, impact of pathogen-associated molecules from gut translocation and saturated fatty acid. *Front. Immunol.* **11**, 613095
- 27 Siwaponanan, P., Siegers, J.Y., Ghazali, R., Ng, T., McColl, B., Ng, G.Z. et al. (2017) Reduced PU.1 expression underlies aberrant neutrophil maturation and function in beta-thalassemia mice and patients. *Blood* **129**, 3087–3099, <https://doi.org/10.1182/blood-2016-07-730135>

- 28 Thim-Uam, A., Surawut, S., Issara-Amphorn, J., Jaroonwichawan, T., Hiengrach, P., Chatthanathon, P. et al. (2020) Leaky-gut enhanced lupus progression in the Fc gamma receptor-1b deficient and pristane-induced mouse models of lupus. *Sci. Rep.* **10**, 777, <https://doi.org/10.1038/s41598-019-57275-0>
- 29 Hiengrach, P., Panpetch, W., Worasilchai, N., Chindamporn, A., Tumwasorn, S., Jaroonwichawan, T. et al. (2020) administration of *Candida albicans* to dextran sulfate solution treated mice causes intestinal dysbiosis, emergence and dissemination of intestinal *Pseudomonas aeruginosa* and lethal sepsis. *Shock* **53**, 189–198, <https://doi.org/10.1097/SHK.0000000000001339>
- 30 Kim, J.J., Shajib, M.S., Manocha, M.M. and Khan, W.I. (2012) Investigating intestinal inflammation in DSS-induced model of IBD. *J. Vis. Exp.* **60**, e3678, <https://doi.org/10.3791/3678>
- 31 Issara-Amphorn, J., Somboonna, N., Pisitkun, P., Hirankarn, N. and Leelahavanichkul, A. (2020) Syk inhibitor attenuates inflammation in lupus mice from FcγRIIb deficiency but not in pristane induction: the influence of lupus pathogenesis on the therapeutic effect. *Lupus* **29**, 1248–1262, <https://doi.org/10.1177/0961203320941106>
- 32 Putt, K.K., Pei, R., White, H.M. and Bolling, B.W. (2017) Yogurt inhibits intestinal barrier dysfunction in Caco-2 cells by increasing tight junctions. *Food Funct.* **8**, 406–414, <https://doi.org/10.1039/C6FO01592A>
- 33 La Carpiá, F., Wojczyk, B., Rebbaa, A., Tang, A. and Hod, E.A. (2016) Chronic transfusion and iron overload modify the mouse gut microbiome. *Am. Soc. Hematol.* **5**, 2270–2285, <https://doi.org/10.1182/blood.V128.22.200.200>
- 34 Yilmaz, B. and Li, H. (2018) Gut microbiota and iron: the crucial actors in health and disease. *Pharmaceuticals (Basel)* **11**, 98, <https://doi.org/10.3390/ph11040098>
- 35 Wexler, H.M. (2007) Bacteroides: the good, the bad, and the nitty-gritty. *Clin. Microbiol. Rev.* **20**, 593–621, <https://doi.org/10.1128/CMR.00008-07>
- 36 San-Juan-Vergara, H., Zurek, E., Ajami, N.J., Mogollon, C., Pena, M., Portnoy, I. et al. (2018) A Lachnospiraceae-dominated bacterial signature in the fecal microbiota of HIV-infected individuals from Colombia, South America. *Sci. Rep.* **8**, 4479, <https://doi.org/10.1038/s41598-018-22629-7>
- 37 Loubinoux, J., Bronowicki, J.-P., Pereira, I.A., Mougénel, J.-L. and Le Faou, A.E. (2002) Sulfate-reducing bacteria in human feces and their association with inflammatory bowel diseases. *FEMS Microbiol. Ecol.* **40**, 107–112, <https://doi.org/10.1111/j.1574-6941.2002.tb00942.x>
- 38 Verstreken, I., Laleman, W., Wauters, G. and Verhaegen, J. (2012) Desulfovibrio desulfuricans bacteremia in an immunocompromised host with a liver graft and ulcerative colitis. *J. Clin. Microbiol.* **50**, 199–201, <https://doi.org/10.1128/JCM.00987-11>
- 39 Meehan, C.J. and Beiko, R.G. (2014) A phylogenomic view of ecological specialization in the Lachnospiraceae, a family of digestive tract-associated bacteria. *Genome Biol. Evol.* **6**, 703–713, <https://doi.org/10.1093/gbe/evu050>
- 40 Williams, J.M., Duckworth, C.A., Burkitt, M.D., Watson, A.J.M., Campbell, B.J. and Pritchard, D.M. (2015) Epithelial cell shedding and barrier function: a matter of life and death at the small intestinal villus tip. *Vet. Pathol.* **52**, 445–455, <https://doi.org/10.1177/0300985814559404>
- 41 Farmakis, D., Giakoumis, A., Aessopos, A. and Polymeropoulos, E. (2003) Pathogenetic aspects of immune deficiency associated with β thalassemia. *Med. Sci. Monit.* **9**, RA19–RA22
- 42 Walker, Jr, E.M. and Walker, S.M. (2000) Effects of iron overload on the immune system. *Ann. Clin. Lab. Sci.* **30**, 354–365
- 43 Wanachiwanawin, W., Wiener, E., Siripanyaphinyo, U., Chinprasertsuk, S., Mawas, F., Fucharoen, S. et al. (1999) Serum levels of tumor necrosis factor-α, interleukin-1, and interferon-γ in beta-thalassemia/HbE and their clinical significance. *J. Interferon Cytokine Res.* **19**, 105–111, <https://doi.org/10.1089/107999099314243>
- 44 Leelahavanichkul, A., Huang, Y., Hu, X., Zhou, H., Tsuji, T., Chen, R. et al. (2011) Chronic kidney disease worsens sepsis and sepsis-induced acute kidney injury by releasing High Mobility Group Box Protein-1. *Kidney Int.* **80**, 1198–1211, <https://doi.org/10.1038/ki.2011.261>
- 45 Doi, K., Leelahavanichkul, A., Hu, X., Sidransky, K.L., Zhou, H., Qin, Y. et al. (2008) Pre-existing renal disease promotes sepsis-induced acute kidney injury and worsens outcome. *Kidney Int.* **74**, 1017–1025, <https://doi.org/10.1038/ki.2008.346>
- 46 Sukhbaatar, N. and Weichhart, T. (2018) Iron regulation: macrophages in control. *Pharmaceuticals (Basel)* **11**, 137, <https://doi.org/10.3390/ph11040137>
- 47 Foster, S.L., Richardson, S.H. and Failla, M.L. (2001) Elevated iron status increases bacterial invasion and survival and alters cytokine/chemokine mRNA expression in Caco-2 human intestinal cells. *J. Nutr.* **131**, 1452–1458, <https://doi.org/10.1093/jn/131.5.1452>
- 48 Wu, M.H., Pan, T.M., Wu, Y.J., Chang, S.J., Chang, M.S. and Hu, C.Y. (2010) Exopolysaccharide activities from probiotic bifidobacterium: immunomodulatory effects (on J774A.1 macrophages) and antimicrobial properties. *Int. J. Food Microbiol.* **144**, 104–110, <https://doi.org/10.1016/j.ijfoodmicro.2010.09.003>
- 49 Gao, K., Wang, C., Liu, L., Dou, X., Liu, J., Yuan, L. et al. (2017) Immunomodulation and signaling mechanism of *Lactobacillus rhamnosus* GG and its components on porcine intestinal epithelial cells stimulated by lipopolysaccharide. *J. Microbiol. Immunol. Infect.* **50**, 700–713, <https://doi.org/10.1016/j.jmii.2015.05.002>